Environmental Science & Technology

Article

Cite This: Environ. Sci. Technol. 2019, 53, 14204−14211

pubs.acs.org/est

Observations and Simulations of Microplastic Debris in a Tide, Wind, and Freshwater-Driven Estuarine Environment: the Delaware Bay

Jonathan H. Cohen,*[,†] Anna M. Internicola,[†] R. Alan Mason,[‡] and Tobias Kukulka[‡]

[†]School of Marine Science and Policy, College of Earth, Ocean and Environment, University of Delaware, Lewes, Delaware 19958, United States

[‡]School of Marine Science Policy, College of Earth, Ocean, and Environment, University of Delaware, Newark, Delaware 19716, United States

Supporting Information

ABSTRACT: Microplastic (MP) in estuarine and coastal environments remains poorly characterized, despite the importance of these physically dynamic regions as a buffer between land, freshwater environments, and the open ocean where plastic debris accumulates. We sampled MP particles to determine concentration, size, and type in Delaware Bay and numerically simulated transport and distribution at a high spatiotemporal resolution of positively buoyant particles, representing common MP types. Baywide MP concentrations averaged between 0.19 and 1.24 pieces m^{-3} depending on size fraction (300−1000 and 1000−5000 μm) and sampling month (April and June 2017). Upper bay stations, which are located in or near the estuarine turbidity maximum, had higher MP concentrations than lower bay and New Jersey shore stations. Fragments were predominately polyethylene, and filaments predominately polypropylene. Model results suggest that buoyant particles quickly (i.e., within hours) organize in patchy, highly inhomogeneous distributions, creating "hot spots" of MP. In the presence of variable currents driven by buoyancy, wind, and tides, we predict high spatial and temporal variability of MP distributions in Delaware Bay; MP concentrations could vary by a factor of 1000 within a tidal cycle at our sample locations. Collectively, these observations and simulations provide a baseline of MP concentrations in Delaware Bay along with broader, contextual understanding for how measurements reflect MP concentrations in a dynamic estuarine system.

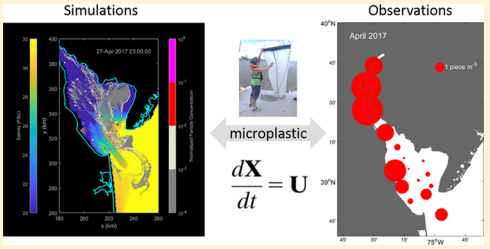

INTRODUCTION

Plastic marine debris is an emerging pollutant of concern globally.[1,2] About 8 million metric tons of plastic were input globally into the ocean in 2010 largely due to coastal waste mismanagement.[3] Microplastic (MP) in the marine environment occurs in sizes below 5 mm and is the most abundant form of marine debris observed at the ocean surface.[1,4] Previous studies suggest that MP presents serious hazards to individual marine organisms.[1,5] Plastic marine debris often begins as land-derived waste, entering estuaries and the coastal ocean. By providing unique habitat and nutrient resources, these coastal regions support rich ecosystems and high biological productivity. Thus, it is anticipated that biological interactions with MP will occur more often in coastal regions than in the open ocean, influencing MP fate and transport.[6]

Surprisingly, few studies have focused on MP in estuarine and coastal waters, despite the high likelihood for plastic accumulation in these regions.[7] From studies in US estuaries and the Great Lakes,[8−10] MP occur in concentrations at or greater than those observed in much of the open ocean.[1] Here, we focus on MP in the Delaware Bay, which is well mixed about south of 39°15′ (Figure 1), i.e., density does not change with depth.[11] Delaware Bay is fed by the Delaware River, whose yearly average river discharge totals 330 m^3 s^{-1}.[1,11] The Delaware River extends from New York state to Delaware Bay and is the longest undammed river east of the Mississippi River, providing drinking water to ∼13 million people, including major cities of Philadelphia and New York City.

The buoyancy-, wind-, and tide-driven estuarine circulation within Delaware Bay likely controls physical transport of marine debris. Tidal currents are strong with maximum speeds of about 1 ms^{-1} in the deep channel.[12] The Delaware Bay is a wide estuary, so that freshwater separates toward the Delaware shore due to Earth's rotation, resulting in buoyancy-driven flows and freshwater river plumes, whose water properties and dynamics are affected by freshwater.[13,14]

Applying both observations of MP in Delaware Bay and model simulations of finer-scale MP distributions as described in Materials and Methods, we provide a baseline of MP concentrations along with contextual understanding for how these point measurements reflect MP concentrations in a dynamic estuarine system through an integrated Results and Discussion section.

Received: August 8, 2019
Revised: November 7, 2019
Accepted: November 8, 2019
Published: November 8, 2019

DOI: 10.1021/acs.est.9b04814
Environ. Sci. Technol. 2019, 53, 14204−14211

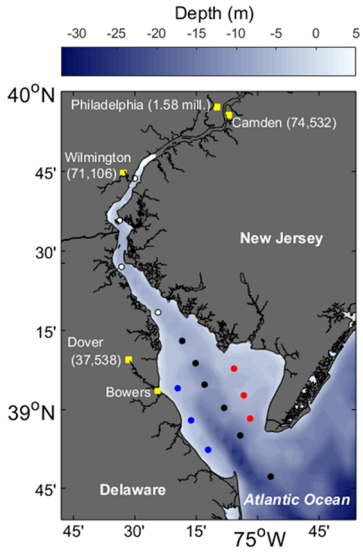

Figure 1. Delaware Bay sampling stations. Stations (n = 16) were sampled, including 4 stations in the estuarine turbidity maximum region (ETM; white circles), 6 stations in the main channel of the lower bay (Bay; black circles), 3 stations along the Delaware shore of the bay (DE-shore; blue circles), and 3 stations along the New Jersey shore of the bay (NJ-shore; red circles). Major cities in the watershed (yellow squares) and their populations are indicated. The town of Bowers, DE, where the Murderkill and St. Jones Rivers enter Delaware Bay, is also shown.

MATERIALS AND METHODS

Observations: MP Collection and Processing. We sampled 16 stations throughout Delaware Bay for MP in April (21st, 28th) and June (12th, 13th) 2017 (Figure 1). Observations were mainly taken a few hours before and after high tide, except on the field day of 4/21, which includes mainly the low-tide phase (Figure S3). The relation between observations and the tidal cycle is discussed in more detail below. The main channel from 11 km outside the bay mouth in the Atlantic Ocean to tidal freshwater near Wilmington, DE was followed by 10 stations. An additional 3 stations were located along the Delaware shoreline adjacent to tributaries (Broadkill River, Mispillion River, and Murderkill/St. Jones Rivers), and another three were located along the New Jersey shoreline adjacent to tributaries (Maurice River, West Creek/Dennis Creek) and Cape May. At each station, we conducted a 5 min surface tow using a ring plankton net (1 m diameter, 200 μm mesh) fitted with a flow meter (General Oceanics) to quantify volume sampled according to manufacturer's instructions (mean [±sd]: April = 292 m^3 [±59]; June 259 m^3 [±29]). Vessel speed was adjusted to maintain the top of the ring just above the sea surface. We transferred samples to glass jars and immediately fixed the collection with 4% formaldehyde. In addition to MP samples, at each station, we obtained water column profiles of temperature, salinity, turbidity, and chlorophyll fluorescence (SeaBird SBE19 CTD, Figure S1).

To isolate MP from the organic material in the plankton net samples, we used wet peroxide oxidation (WPO) and density separation.[15] The total sample was size-fractionated on nitex mesh sieves (>5000 μm; 5000−1000 μm; 1000−300 μm). The two smaller size fractions were then dried overnight at 90 °C and subjected to the WPO/density separation protocol. Material collected from density separators contained putative MP along with some organic/inorganic debris. These were collected onto 200 μm nitex mesh and wrapped in an aluminum foil to dry. We then enumerated MP from these samples by manual examination under a stereomicroscope, followed by confirming MP designations with a hot needle test and assigning each piece of MP to a plastic type (i.e., fragments, filaments, pellets, and other [films, foams, etc.]).[16]

MP concentrations (number of MP pieces m^{-3}) for a given station were calculated based on MP pieces enumerated in that sample, divided by the net-filtered water volume. For statistical analyses, we tested size-fractionated (300−1000 and 1000−5000 μm) MP concentrations separately. We included a grouping of stations according to the region of the estuary: (1) estuarine turbidity maximum (ETM; as defined previously[11] n = 4 stations), (2) Delaware Bay main channel (Bay; n = 6 stations), (3) Delaware shore of Delaware Bay (DE-shore; n = 3 stations), and (4) New Jersey shore of Delaware Bay (NJ-shore; n = 3 stations) (Figure 1). We conducted a 3-factor analysis of variance (ANOVA) for each MP concentration, with month, estuarine region, and MP type as factors. Data were transformed (log[1 + MP concentration]) prior to analysis.

To determine the most common plastic formulations in our samples, we conducted attenuated total reflectance (ATR) Fourier transform infrared (FTIR) spectroscopy. We subsampled 1−4 MP pieces per station for both April and June 2017 (167 pieces total), which represented 1.8% of all MP collected. The microplastics chosen for this analysis were representative of the majority of MP in the sample and were deemed large enough to give reliable spectra with our instrumentation (approx. >500 μm). We collected FTIR spectra (32 scans at 4 cm^{-1}) with a Thermo Nicolet Nexus spectrometer using single bounce ATR-FTIR spectroscopy (Smart Orbit, Thermo) with a diamond internal reflection element. We used SpectraGryph 1.2 software to compare all acquired spectra against a library of plastic standards for MP analysis.[17] Following previous work[18] we truncated these reference spectra to 1250−3600 cm^{-1} wavenumbers. We accepted a plastic identification for a given MP piece that achieved the highest percentage match to a reference standard, provided that the match was greater than 80%, otherwise the piece was considered "unknown". We compared plastic formulation between seasons, size fractions, and among MP types with chi-square tests.

Simulations: Numerical Modeling. As a first step to understand the spatiotemporal variability of buoyant MP in Delaware Bay, we tracked surface-trapped particles in a hydrodynamic model following previous approaches.[19] We performed hydrodynamic simulations of three-dimensional, time-dependent currents and salinity in and near Delaware Bay, applying an existing, validated hydrodynamic model[20] based on a coupled application of the regional ocean modeling system (ROMS)[21,22] within the Coupled-Ocean-Atmospheric-Wave-Sediment Transport (COAWST) Modeling System.[23] Similar regional ocean circulation models have been successfully applied previously to the Delaware Bay and its adjacent continental shelf.[13,24−26]

Our computational domain included the Delaware Bay, parts of the upper estuary, and extended to the continental shelf break. The grid was regular curvilinear with the highest resolution near the bay mouth at 0.75−2.0 km and the lowest grid resolution near the shelf break with a grid spacing of about 8 km, which is adequate to resolve key circulation processes. The model captured realistically tide-, wind-, and buoyancy-driven circulation, whose corresponding forcings were imposed.[20]

The hydrodynamic model was spun up for several months, starting in September 2016, and run for the full field sampling

DOI: 10.1021/acs.est.9b04814
Environ. Sci. Technol. 2019, 53, 14204−14211

Table 1. MP Concentrations in Delaware Bay[a]

		MP [pieces m^{-3}]		MP [pieces km^{-2}]	
month	size fraction [μm]	MP conc. (SE)	range [min−max]	MP conc. (SE)	range [min−max]
April	300−1000	0.87 (0.20)	0.12−2.94	6.8×10^5 (1.5×10^5)	9.5×10^4−2.3×10^6
	1000−5000	0.37 (0.11)	0.04−1.67	2.9×10^5 (8.7×10^4)	3.0×10^4−1.3×106
	300−5000	1.24 (0.26)	0.19−3.33	1.1×10^6 (2.2×10^5)	2.9×10^5−2.9×10^6
June	300−1000	0.42 (0.15)	0.06−2.36	3.3×10^5 (1.2×10^5)	5.0×10^4−1.9×10^6
	1000−5000	0.19 (0.15)	0.00−2.45	1.5×10^5 (1.2×10^5)	0−1.9×10^6
	300−5000	0.62 (0.29)	0.07−4.81	4.9×10^5 (2.3×10^5)	5.8×10^4−3.8×10^6

[a]All stations (n = 16) in a given sampling month are treated as replicates. Mean MP concentration (± standard error (SE)) and the range among stations are provided per volume (pieces m^{-3}) and per area (pieces km^{-2}) for small (300−1000 μm), large (1000−5000 μm), and total (300−5000 μm) size fractions.

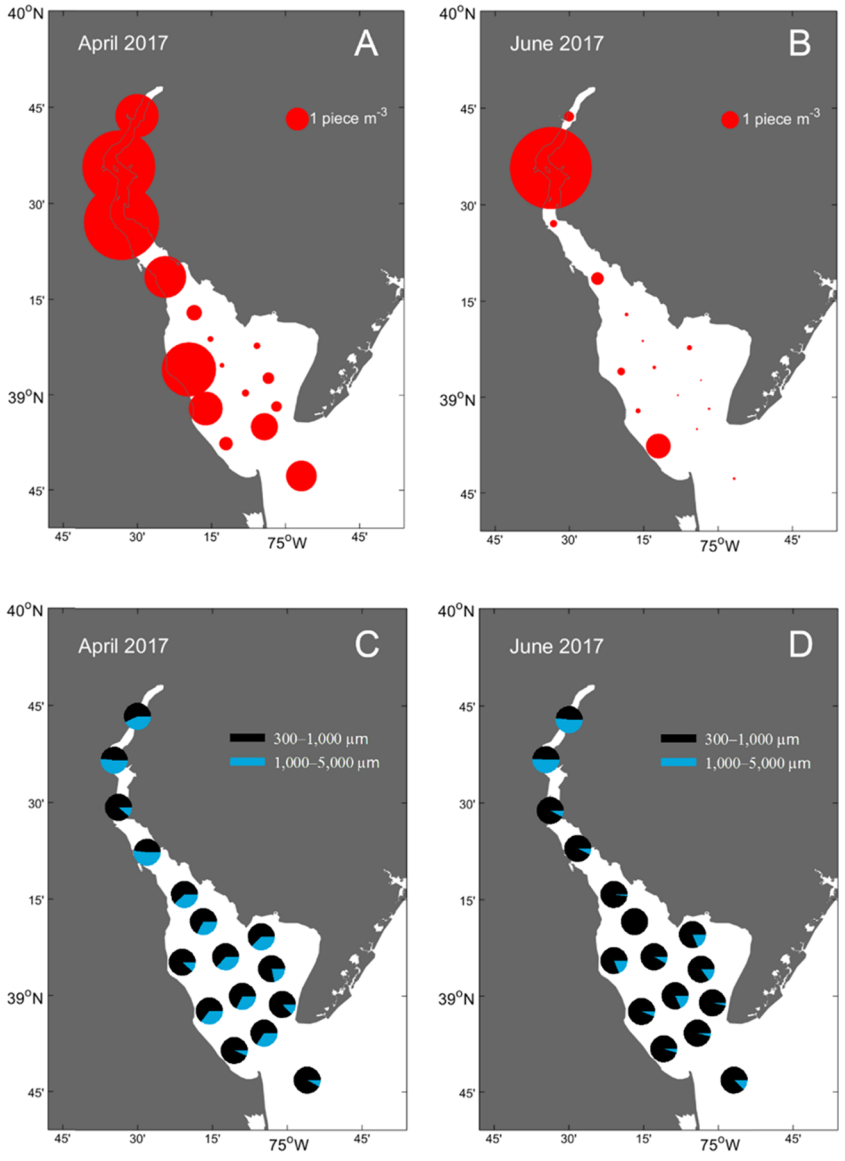

Figure 2. Concentration of MP in Delaware Bay. Concentration of MP (pieces m^{-3}) from combined size fractions (300−5000 μm) is represented by the size of each circle for (A) April and (B) June sampling. (C, D) Relative abundance of the small (black) and large (blue) size fractions for April and June sampling, respectively.

period. Surface-trapped particles were released at several time points during the sampling period to understand where, when, and how particles move within the Bay, exit the Bay, or accumulate in surface convergence regions. Each release consisted of over a million particles that are initially homogeneously distributed within the Delaware Bay. Note that our approach neither takes into account most likely particle sources nor the range of particle buoyant rise velocities, because those are currently unknown for Delaware Bay and challenging to determine in field conditions.[26−28] This greatly simplifies the

DOI: 10.1021/acs.est.9b04814
Environ. Sci. Technol. 2019, 53, 14204−14211

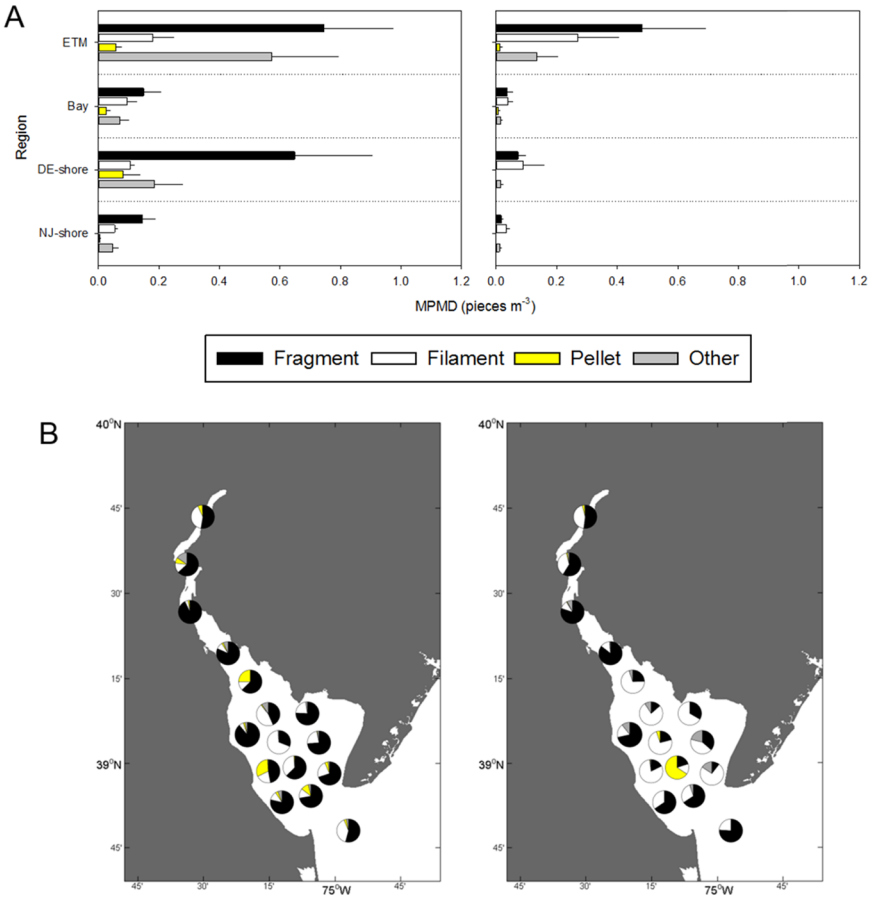

Figure 3. Distribution of MP types in Delaware Bay. (A) Means (pieces m^{-3} ± standard error) for each MP type within each estuary region, where stations within each region and season are treated as replicates (ETM, $n = 8$; Bay, $n = 12$; DE-shore, $n = 6$; NJ-shore, $n = 6$). (B) Relative composition of MP types in samples from each station for the small size fraction (300−1000 μm; left panel) and the large size fraction (100−5000 μm; right panel).

problem because not-well understood turbulent downward mixing of MP[19] does not need to be represented in the model, which is consistent with our modeling goals; however, care must be taken in comparing simulations with observations. The tide and river discharge conditions during the April and June 2017 field experiments were sufficiently similar with maximum tidal amplitudes of about 1 m and Delaware River discharge at Trenton, New Jersey, between 300 and 400 $m^3\ s^{-1}$, so that we discuss in detail below only the April 2017 simulation results, which suffices for the qualitative comparison with observations below. Wind speed and direction are overall relatively constant over the study period with relatively weak wind speeds of less than 5 ms^{-1}. An exception is the last field day of 6/13/17 when wind speeds increase moderately to about 6−8 ms^{-1} at the end of the field day. Therefore, our discussion focuses on tidal variability. Rather than a direct comparison with observations, our simulation approach is aimed at understanding the expected MP variability due to MP transport by surface currents in a dynamic coastal environment and to facilitate the interpretation of observations.

RESULTS AND DISCUSSION

Observations: MP Particles are Ubiquitous but Vary by Region and Type. Baywide MP concentrations (300−5000 μm) varied, on average, between 0.19 and 1.24 pieces m^{-3} (1.5×10^5−1.1×10^6 pieces km^{-2}) depending on size fraction and sampling month (Table 1, Figures 2 and S2). While higher than typical values reported for the open ocean,[29,30] these MP concentrations are comparable to those in urban rivers of the Chicago metropolitan area (2.4 pieces m^{-3})[31] and two urbanized tributaries of Chesapeake Bay (~1×10^5 pieces km^{-2})[9], both studies using similar operational definitions of MP and processing methods as used in our study.

Considering the two size fractions in more detail, we observed seasonal differences in MP concentration in Delaware Bay surface water, but this depended on size fraction (Figures 2 and S2). Baywide, MP concentrations for the small size fraction (300−1000 μm) in April exceeded those in June ($P = 0.004$, the effect of the month in 3-way ANOVA; $P = 0.004$, Holm-Sidak post-hoc test). However, baywide MP concentration for the large (100−5000 μm) size fraction did not differ between months ($P = 0.067$, the effect of the month in 3-way ANOVA). Because tidal currents are significant in Delaware Bay, it is interesting to compare our observations to tidal elevation (Figure S3). However, we find no obvious relation between MP observations and tidal phase. Our model results discussed below suggest that this is because MP observations are not sampled at sufficiently high space and time resolution for observing tidal variability.

We observed an interaction between region (ETM/Bay/DE-shore/NJ-shore) and type (fragment/filament/pellet/other) in both the small and large fractions (3-way ANOVA region x type, $P = 0.015$ and 0.041, respectively) (Figure 3). Thus, MP concentration varied among Delaware Bay regions within MP types. For the small size fraction, both ETM and DE-shore regions had more fragments than Bay and NJ-shore regions,

DOI: 10.1021/acs.est.9b04814
Environ. Sci. Technol. 2019, 53, 14204−14211

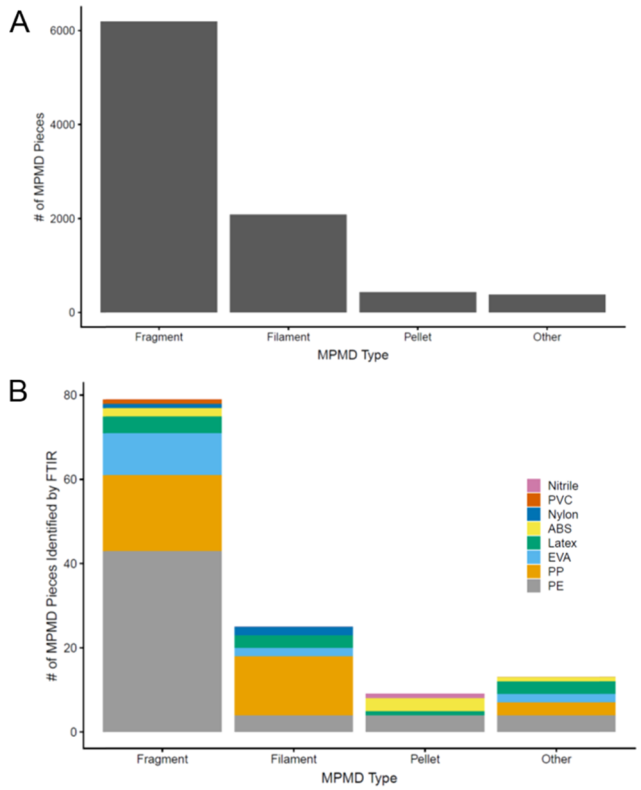

Figure 4. MP types and identified plastic formulations. (A) MP types for all pieces collected during Delaware Bay sampling. (B) A subsample of these pieces (n = 167) identified to their plastic formulations by ATR-FTIR. Out of the 167 pieces, 126 had a spectral match greater than 80%, representing 1.4% of all MP collected in the study. Abbreviations: PVC = poly(vinyl chloride); ABS = acrylonitrile butadiene styrene; EVA = ethylene vinyl acetate; PP = polypropylene; PE = polyethylene.

while ETM also had more "other" types than Bay and NJ-shore (Figure 3A and Table S1). We did not find differences among regions for either filaments or pellets for the small size fraction. For the large size fraction, fragment concentration was higher in the ETM region than in all others, while filament concentration in the ETM also exceeded that at Bay stations (Figure 3A and Table S1). It is useful to also consider MP distribution in Delaware Bay in terms of the relative contribution of each MP type at a given station (Figure 3B). Fragments dominated the samples at most stations, but filaments had high relative abundance at lower bay stations, particularly in the larger size fraction. In contrast, pellets were highly localized in their distribution, dominating at one or two stations depending on size fraction (Figure 3B), which could be due to a local source event. The predominance of fragments, and to a lesser extent filament, can also be seen when comparing MP types of all pieces collected during this study (Figure 4A). A previous study[10] similarly found fragments to dominate their sampling of two estuaries in the southeastern US.

Through ATR-FTIR analysis of a subsample of our MP pieces (Figure 4B), we found no statistically significant difference in the plastic formulation of the MP collected from the four Delaware Bay regions ($\chi_{12,n=121}^2$ = 7.508, P = 0.8223). However, plastic formulation did vary among: (1) season ($\chi_{4,n=121}^2$ = 19.772, P < 0.001) with less ABS and EVA in April than June; (2) size ($\chi_{4,n=121}^2$ = 9.8756, P = 0.04258) with less latex in the small size fraction than in the large; and (3) MP type ($\chi_{12,n=121}^2$ = 43.122, P < 0.001) with polyethylene dominating fragments and polypropylene dominating filaments (54 and 56% of those types identified, respectively). Given the abundance of fragments and filaments in our samples overall, polyethylene and polypropylene are likely the most common plastic formulations in Delaware Bay, as observed in other river/estuary systems.[31] MP of these formulations is positively buoyant to varying degrees.[27]

Simulations: Surface Currents Drive Hot Spots of Particle Distributions. Overall, the observed type (shape), formulation (material), and size distributions of MP are complex and challenging to interpret comprehensively, which is expected given the multifaceted transport and fate of MP in estuaries.[1,7] Given this complexity, our simulation effort focused on one

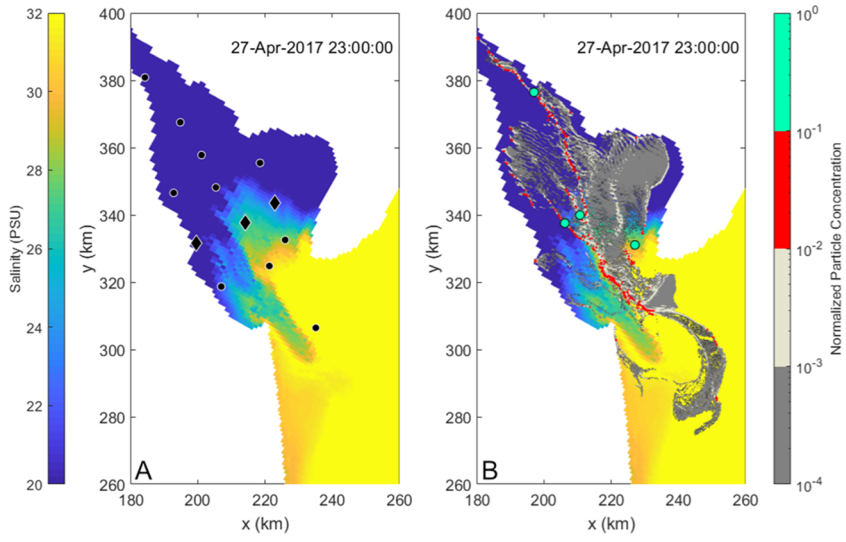

Figure 5. Snapshot of simulated (A) sea surface salinity and (B) particle concentrations on 4/27/2017 at 2300 UTC. Black symbols in (A) show sampling locations from Figure 1. Time series of concentrations are presented in Figure 6 at the locations indicated by diamonds. Concentrations are normalized by the maximum concentration value and normalized concentrations between 0.1 and 1 highlighted by green circles (normalized concentrations below 10^{-5} are not shown).

DOI: 10.1021/acs.est.9b04814
Environ. Sci. Technol. 2019, 53, 14204−14211

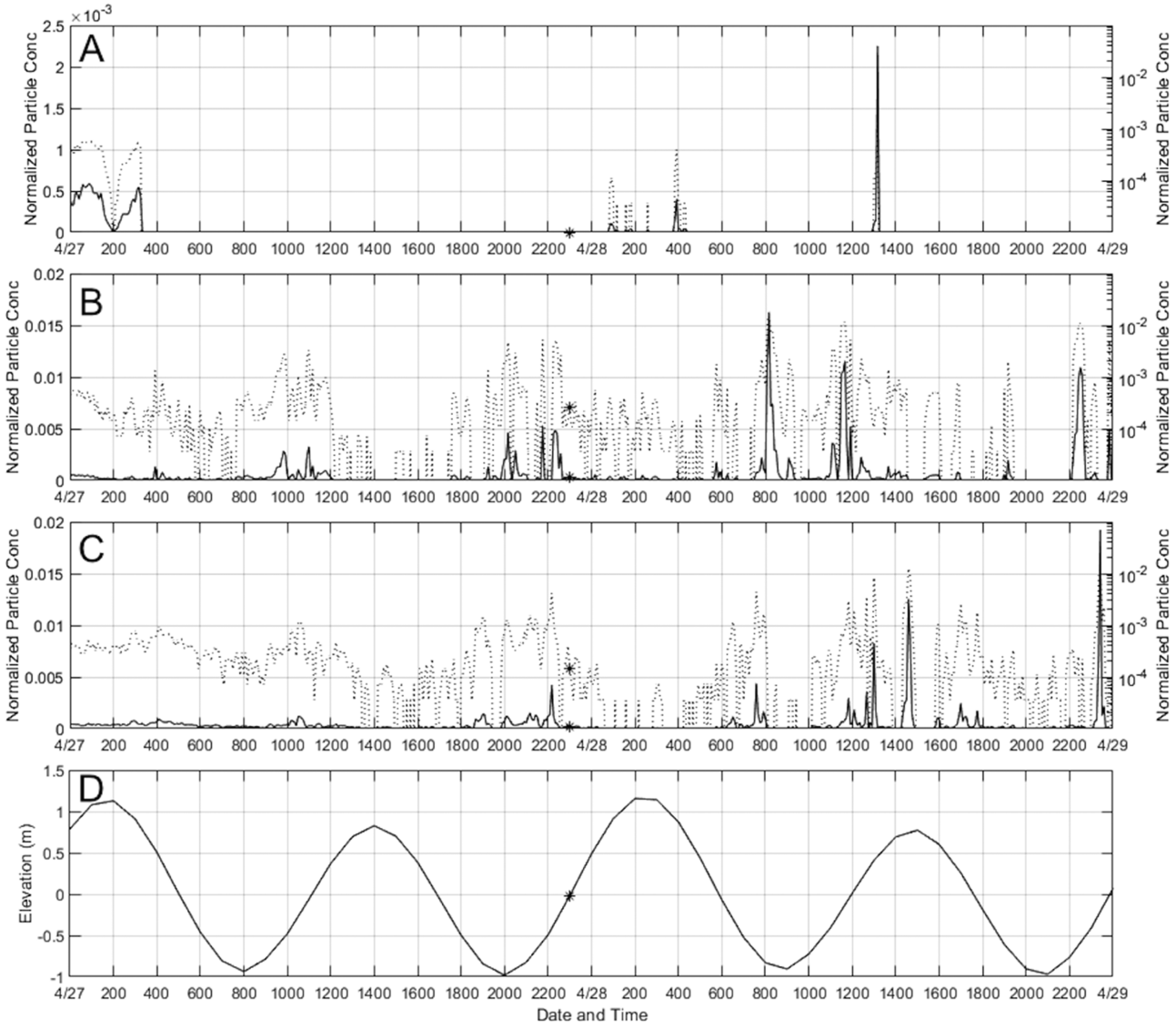

Figure 6. Time series of particle concentrations and tidal elevation. Particle concentrations are normalized by the maximum concentration value and shown in linear (solid line) and logarithmic (dotted line) scales for locations near (A) Delaware shore, (B) mid-bay, and (C) New Jersey shore (compare with black diamonds Figure 5A). (D) Tidal elevation time series at the Delaware mouth close to the Delaware shore. Star indicates the time of snapshot in Figure 5.

rational, straightforward approach, employing numeric surface drifters to illustrate the dynamic estuarine environment and potential consequences for interpreting observations. Thus, our results here will not include a discussion of the ETM that is associated with particle trapping of denser (negatively buoyant) sediments due to flood and ebb asymmetry;[32] but focused work on MP in ETM regions is warranted in a more comprehensive follow-up study.

One striking feature of simulated buoyant particles is that they quickly (after a few hours) organize in patchy, highly inhomogeneous distributions (Figure 5). This is remarkable considering that the particle source was initially homogeneous within Delaware Bay but not entirely unexpected, because multiple mechanisms can lead to fronts and surface convergence in estuaries, which are explained next.[14,33,34] A salinity front is characterized by strong salinity gradients for example just outside the bay mouth and near the deeper channel in the bay. Surface particle organization occurs in thin filaments due to converging surface currents near salinity fronts and subsequent stirring by currents associated with the freshwater plume.[35] For example, note the salinity front close to the southern bay mouth and associated filaments southeast of the bay mouth (Figure 5). Particles also accumulate in narrow rows in the bay close to the deeper channel (see Figure 1 bathymetry) where tidal currents are strong, possibly due to axial convergence in a well-mixed estuary.[36] These rows with high particle concentrations may then be advected away from the channel toward the New Jersey shore, resulting in multiple high-concentration rows of particles (Figure 5). Furthermore, buoyant particles tend to be transported away from the Delaware shore toward the New Jersey shore for the specific wind, tide, river discharge conditions at the end of April 2017. In particular, particle surface concentrations are elevated near and around Cape May, NJ. Our simulations suggest that buoyant particle concentrations vary greatly in space and that particles accumulate in hot spots that are controlled by the surface circulation in and near Delaware Bay.

DOI: 10.1021/acs.est.9b04814
Environ. Sci. Technol. 2019, 53, 14204−14211

In the presence of dynamic surface currents and tidal oscillations, great spatial variability of particle distributions in Delaware Bay implies great temporal variability as well. Our simulations suggest that particle concentrations sampled at fixed locations vary with the tidal cycle (Figure 6). If a particle hot spot is transported by currents through a fixed sample location, particle concentrations may vary by a factor of 1000 over just 30 min, which has critical implications for the interpretation of MP field samples.

Interpretation of Observations in Light of Model Results. Our simulations indicate that care has to be taken in determining observed differences between stations or seasons, e.g., observed seasonal differences between larger size fractions during April and June, because such differences may be partially due to sampling closer or farther away from particle hot spots at a given time (Figure 5). Differences in observed and simulated particle concentrations may also be due to different sampling volumes, which is investigated in the Supporting material (Figure S4). Qualitatively, the coarse-resolution (high sample volume) results are similar to the high-resolution (small sample volume) results, but sharp gradients are smeared due to spatial averaging. A time series of two-dimensional (2D) surface salinity and MP concentrations in Delaware Bay starting on 4/28/2017 illustrates the sensitivity of MP measurements on location and timing over a tidal cycle (Video S1 in the Supporting materials section). The 2D maps include appearing and disappearing measurement locations and timing corresponding to each field station (blue diamonds in Video S1). Clearly, the specific timing and location of each field station relative to MP concentrations, which vary over a tidal cycle, determine whether samples are just inside or outside MP hot spots. Thus, the simulations are valuable for more comprehensive interpretations of our MP observations, which were limited in space and time.

Relatively high observed concentrations near Cape May, NJ, and the Delaware estuary mouth (Figure 2) are at first glance unexpected because river water with higher MP content should mix with cleaner ocean water, resulting in lower MP concentrations closer to the ocean.[10,37] However, simulations indicate that buoyant particles may aggregate near Cape May and the estuary mouth, which could explain the relatively high observed concentrations at those locations.

The comparison of observed and modeled MP distributions may also indicate unidentified MP sources. For example, simulated MP particles are transported away from the Delaware shore, whereas observations reveal significant MP content near the Delaware shore (Figure 5). Thus, relatively high concentrations observed near the Delaware shore (e.g., Figure 2) would imply a local MP source near this location. One such potential source could be tributaries. The Murderkill River receives the outfall from a wastewater treatment plant serving 13 000 people with an average daily flow of 12.5 million gallons per day, while the nearby St. Jones River has 68 323 people in the watershed, which includes the city of Dover, DE. Both tributaries enter Delaware Bay near Bowers, DE (39.06°N, 75.40°W), corresponding to elevated concentrations of MP in the small size fraction in April 2017 (Figure 2, Table 1). Note that those potential MP inputs may also depend on the season, but we have insufficient data to establish a seasonal dependence of our MP observations.

Simulation results also allow an estimate of potential peak MP concentrations near sampling locations by relating observed concentrations (Figure 2) to simulated concentrations (Figures 5 and 6). For example, observed MP concentrations at the two stations closest to the Delaware Bay mouth (Figure 1) are between 7×10^5 and 9×10^5 pieces km^{-2} in April 2017. If these measurements would have been taken near a hot spot (Figures 5 and 6), surrounding MP concentrations would have been much lower. However, if these measurements would have been taken outside the MP hot spots, the combination of model and observations yields peak MP concentrations in hot spots of up to 9×10^{10} pieces km^{-2}, which are much higher than typical values previously reported for the open ocean.[29,30]

Our study observes substantial MP concentration in Delaware Bay, reveals great spatiotemporal variability of MP in the bay, and highlights that MP properties and distributions can strongly depend on the river, wind, and tide conditions, which should be taken into account in future studies of MP in estuaries. Therefore a comprehensive sampling plan must incorporate sufficient spatiotemporal coverage to capture this variability. Interpretation of observed MP concentrations in estuaries should be done cautiously if sampling volume and/or spatial coverage is limited. Ultimately, if we are to understand the spatiotemporal distribution of MP in tide, wind, and freshwater-driven environments like estuaries, the design of subsequent observational studies must consider physical processes that could aggregate MP.

■ ASSOCIATED CONTENT

Supporting Information

The Supporting Information is available free of charge at https://pubs.acs.org/doi/10.1021/acs.est.9b04814.

P-values for Holm-Sidak post-hoc tests comparing Delaware Bay regions, CTD profiles for sampling stations, MP concentration by size fraction, month, and Bay region, the timing of MP sampling relative to tidal height, time series of particle concentrations for coarse- and high-resolution bin sizes, video of simulation results (PDF)

Simulated (left) sea surface salinity and (right) particle concentrations (MOV)

■ AUTHOR INFORMATION

Corresponding Author

*E-mail: jhcohen@udel.edu. Tel.: 302-645-4298.

ORCID

Jonathan H. Cohen: 0000-0002-2032-7874

Author Contributions

J.H.C. and T.K. contributed equally. The manuscript was written through the contributions of all authors. All authors have given approval to the final version of the manuscript.

Notes

The authors declare no competing financial interest.

■ ACKNOWLEDGMENTS

This work was supported by Delaware Sea Grant College Program awards R/HCE-11 and R/HCE31 as well as a private donation for collaborative faculty research to J.H.C. and T.K.; A.M.I. was supported as an REU student by the National Science Foundation under Grant No. 1460963; additional fellowship support was provided by the UD School of Marine Science and Policy to A.M.I. (Program Fellowship) and R.A.M. (Okie Fellowship). H. Glos and J. Steinberg assisted with MP collection and sample processing. We would like to thank two anonymous reviewers for valuable comments that have improved this manuscript.

DOI: 10.1021/acs.est.9b04814
Environ. Sci. Technol. 2019, 53, 14204−14211

ABBREVIATIONS

MP microplastic
ETM estuarine turbidity maximum
ABS acrylonitrile butadiene styrene
EVA ethylene vinyl acetate

REFERENCES

(1) Law, K. L. Plastics in the Marine Environment. *Annu. Rev. Mater. Sci.* **2017**, *9*, 205−229.
(2) Galloway, T. S.; Cole, M.; Lewis, C. Interactions of microplastic debris throughout the marine ecosystem. *Nat. Ecol. Evol.* **2017**, *1*, No. 0116.
(3) Jambeck, J. R.; Geyer, R.; Wilcox, C.; Siegler, T. R.; Perryman, M.; Andrady, A.; Narayan, R.; Law, K. L. Plastic waste inputs from land into the ocean. *Science* **2015**, *347*, 768−771.
(4) *Tech. Memo. NOS-OR&R-30*; Proceedings of the International Research Workshop on the Occurrence, Effects, and Fate of Microplastic Marine Debris, Arthur, C., Arthur, C., Baker, J., Bamford, H., Eds.; National Oceanic and Atmospheric Administration: Washington, DC, 2009.
(5) Syberg, K.; Khan, F. R.; Selck, H.; Palmqvist, A.; Banta, G. T.; Daley, J.; Sano, L.; Duhaime, M. B. Microplastics: Addressing ecological risk through lessons learned. *Environ. Toxicol. Chem.* **2015**, *34*, 945−953.
(6) Clark, J. R.; Cole, M.; Lindeque, P. K.; Fileman, E.; Blackford, J.; Lewis, C.; Lenton, T. M.; Galloway, T. S. Marine microplastic debris: a targeted plan for understanding and quantifying interactions with marine life. *Front. Ecol. Environ.* **2016**, *14*, 317−324.
(7) Vermeiren, P.; Muñoz, C. C.; Ikejima, K. Sources and sinks of plastic debris in estuaries: A conceptual model integrating biological, physical and chemical distribution mechanisms. *Mar. Pollut. Bull.* **2016**, *113*, 7−16.
(8) Eriksen, M.; Mason, S.; Wilson, S.; Box, C.; Zellers, A.; Edwards, W.; Farley, H.; S. Amato, S. Microplastic pollution in the surface waters of the Laurentian Great Lakes. *Mar. Pollut. Bull.* **2013**, *77*, 177−182.
(9) Yonkos, L. T.; Friedel, E. A.; Perez-Reyes, A. C.; Ghosal, S.; Arthur, C. D. Microplastics in four estuarine rivers in the Chesapeake Bay, U.S.A. *Environ. Sci. Technol.* **2014**, *48*, 14195−14202.
(10) Gray, A. D.; Wertz, H.; Leads, R. R.; Weinstein, J. E. Microplastic in two South Carolina Estuaries: Occurrence, distribution, and composition. *Mar. Pollut. Bull.* **2018**, *128*, 223−233.
(11) Sommerfield, C. K.; Wong, K.-C. Mechanisms of sediment flux and turbidity maintenance in the Delaware Estuary. *J. Geophys. Res.* **2011**, *116*, No. C01005.
(12) Wünchow, A.; Masse, A. K.; Garvine, R. W. Astronomical and nonlinear tidal currents in a coupled estuary shelf system. *Cont. Shelf Res.* **1992**, *12*, 471−498.
(13) Whitney, M. M.; Garvine, R. W. Wind influence on a coastal buoyant outflow. *J. Geophys. Res.* **2005**, *110*, No. C03014.
(14) Horner-Devine, A. R.; Hetland, R. D.; MacDonald, D. G. Mixing and transport in coastal river plumes. *Annu. Rev. Fluid Mech.* **2015**, *47*, 569−594.
(15) Masura, J.; Baker, J.; Foster, G.; Arthur, C. *Laboratory Methods for the Analysis of Microplastics in the Marine Environment: Recommendations for Quantifying Synthetic Particles in Waters and Sediments*; NOAA Technical Memorandum NOS-OR&R-48, National Oceanic and Atmospheric Administration: Washington, DC, 2015.
(16) Hidalgo-Ruz, V.; Gutow, L.; Thompson, R. C.; Thiel, M. Microplastics in the marine environment: A review of the methods used for identification and quantification. *Environ. Sci. Technol.* **2012**, *46*, 3060−3075.
(17) Jung, M. R.; Horgen, F. D.; Orski, S. V.; Rodriguez, V.; Beers, K. L.; Balazs, G. H.; Jones, T. T.; Work, T. M.; Brignac, K. C.; Royer, S.-J.; Hyrenbach, K. D.; Jensen, B. A.; Lynch, J. M. Validation of ATR FT-IR to identify polymers of plastic marine debris, including those ingested by marine organisms. *Mar. Pollut. Bull.* **2018**, *127*, 704−716.
(18) Primpke, S.; Wirth, M.; Lorenz, C.; Gerdts, G. Reference database design for the automated analysis of microplastic samples based on Fourier transform infrared (FTIR) spectroscopy. *Anal. Bioanal. Chem.* **2018**, *410*, 5131−5141.
(19) Kukulka, T.; Brunner, K. Passive buoyant tracers in the ocean surface boundary layer: 1. Influence of equilibrium wind-waves on vertical distributions. *J. Geophys. Res.: Oceans* **2015**, *120*, 3837−3858.
(20) Kukulka, T.; Jenkins, R. L.; Kirby, J. T.; Shi, F.; Scarborough, R. W. Surface wave dynamics in Delaware Bay and its adjacent coastal shelf. *J. Geophys. Res.: Oceans* **2017**, *122*, 8683−8706.
(21) Haidvogel, D. B.; Arango, H. G.; Hedstrom, K.; Beckmann, A.; Malanotte-Rizzoli, P.; Shchepetkin, A. F. Model evaluation experiments in the North Atlantic Basin: Simulations in nonlinear terrain-following coordinates. *Dyn. Atmos. Oceans* **2000**, *32*, 239−281.
(22) Shchepetkin, A. F.; Mcwilliams, J. C. The regional oceanic modeling system (ROMS): a split-explicit, free-surface, topography-following-coordinate oceanic model. *Ocean Modell.* **2005**, *9*, 347−404.
(23) Warner, J. C.; Armstrong, B.; He, R.; Zambon, J. B. Development of a Coupled Ocean−Atmosphere−Wave−Sediment Transport (COAWST) Modeling System. *Ocean Modell.* **2010**, *35*, 230−244.
(24) Hofmann, E.; Bushek, D.; Ford, S.; Guo, X.; Haidvogel, D.; Hedgecock, D.; Klinck, J.; Milbury, C.; Narvaez, D.; Powell, E.; Wang, Y.; Wang, Z.; Wilkin, J.; Zhang, L. Understanding how disease and environment combine to structure resistance in estuarine bivalve populations. *Oceanography* **2009**, *22*, 212−231.
(25) Aristizábal, M.; Chant, R. A numerical study of salt fluxes in Delaware Bay Estuary. *J. Phys. Oceanogr.* **2013**, *43*, 1572−1588.
(26) Reisser, J.; Slat, B.; Noble, K.; du Plessis, K.; Epp, M.; Proietti, M.; de Sonneville, J.; Becker, T.; Pattiaratchi, C. The vertical distribution of buoyant plastics at sea: An observational study in the North Atlantic Gyre. *Biogeosciences* **2015**, *12*, 1249−1256.
(27) Waldschläger, K.; Schüttrumpf, H. Effects of particle properties on the settling and rise velocities of microplastics in freshwater under laboratory conditions. *Environ. Sci. Technol.* **2019**, *53*, 1958−1966.
(28) Kooi, M.; Besseling, E.; Kroeze, C.; van Wenzel, A. P.; Koelmans, A. A. Modeling the fate and transport of plastic debris in freshwaters: review and guidance. In *Freshwater Microplastics*; Wagner, M.; Lambert, S., Eds.; Springer: Cham, 2018.
(29) Law, K. L.; Mort-Ferguson, S. E.; Maximenko, N. A.; Proskurowski, G.; Peacock, E. E.; Hafner, J.; Reddy, C. M. Plastic accumulation in the North Atlantic Subtropical Gyre. *Science* **2010**, *329*, 1185−1188.
(30) Law, K. L.; Mort-Ferguson, S. E.; Goodwin, D. S.; Zettler, E. R.; DeForce, E.; Kukulka, T.; Proskurowski, G. Distribution of surface plastic debris in the eastern Pacific Ocean from an 11-year data set. *Environ. Sci. Technol.* **2014**, *48*, 4732−4738.
(31) McCormick, A. R.; Hoellein, T. J.; London, M. G.; Hittie, J.; Scott, J. W.; Kelly, J. J. Microplastic in surface waters of urban rivers: concentration, sources, and associated bacterial assemblages. *Ecosphere* **2016**, *7*, No. e01556.
(32) Jay, D. A.; Musiak, J. D. Particle trapping in estuarine tidal flows. *J. Geophys. Res.* **1994**, *99*, 20445−20461.
(33) O'Donnell, J. Surface fronts in estuaries: A review. *Estuaries* **1993**, *16*, 12−39.
(34) MacCready, P.; Geyer, W. R. Advances in estuarine physics. *Annu. Rev. Mater. Sci.* **2010**, *2*, 35−58.
(35) Whitney, M. M.; Garvine, R. W. Simulating the Delaware Bay buoyant outflow: Comparison with observations. *J. Phys. Oceanogr.* **2006**, *36*, 3−21.
(36) Nunes, R. A.; Simpson, J. H. Axial convergence in a well-mixed estuary. *Estuarine, Coastal Shelf Sci.* **1985**, *20*, 637−649.
(37) Luo, W.; Su, L.; Craig, N. J.; Du, F.; Wu, C.; Shi, H. Comparison of microplastic pollution in different water bodies from urban creeks to coastal waters. *Environ Poll.* **2019**, *246*, 174−182.

DOI: 10.1021/acs.est.9b04814
Environ. Sci. Technol. 2019, 53, 14204−14211